SPECTRAL MAPPING OF ALTERATION PHASES WITHIN A HYDROTHERMAL VUG AT THE HAUGHTON IMPACT STRUCTURE. R. N. Greenberger[1], J. F. Mustard[1], G. R. Osinski[2,3], L. L. Tornabene[2,4], C. L. Marion[2], A. Pontefract[2], and E. A. Cloutis[5], [1]Dept. of Geological Sciences, Brown University, Providence, RI, 02912, Rebecca_Greenberger@brown.edu, [2]Dept. of Earth Sciences & Centre for Planetary Science and Exploration, University of Western Ontario, London, ON, N6A 5B7, Canada, [3]Dept. Physics & Astronomy, University of Western Ontario, London, ON, N6A 5B7, Canada, [4]SETI Institute, Mountain View, CA 94043, USA, [5]Dept. of Geography, University of Winnipeg, Winnipeg, MB R3B 2E9, Canada.

Introduction: Meteorite impacts are an important process in the solar system, and post-impact hydrothermal systems can be generated from impacts where water is present [e.g., 1-2]. These impact-generated hydrothermal systems have been proposed to have existed on Mars [e.g., 2-6], and studying impacts on Earth can help advance our understanding of these processes and questions of habitability on Mars. Hydrothermal systems have also been identified as high priority targets for a future Mars sample return mission [7].

The Haughton impact structure is a ~23 Ma complex crater with an apparent diameter of 23 km on Devon Island, Canadian High Arctic, and has been extensively studied to understand impact processes due to its exceptional preservation and exposure [e.g., 8-11]. Deposits from several types of impact-related hydrothermal mineralization have been found at Haughton [8, 12], and we are studying one such outcrop, a calcite-marcasite vug within the impact melt rocks that has been oxidized and weathered in places to sulfates at low temperatures after the hydrothermal system cooled [8, 12-13]. Our goals are to map the mineral assemblages present with hyperspectral imaging and synthesize this information with other measurements to understand the formation and weathering processes.

Methods: The outcrop was imaged during the 2013 field season from distances on the order of meters and tens of meters with a Channel Systems near infrared (NIR) hyperspectral imager covering 0.65-1.1 µm with 10 nm spectral resolution and 10 nm sampling. Images were calibrated through a dark object subtraction and corrected to reflectance using a separate image taken next to the outcrop of Spectralon®. Spectral summary parameters [e.g., 14] were calculated to map spectral features due to differences in Fe oxidation state or coordination environment.

Ten hand samples representative of the major phases present at the outcrop, six of which were within NIR images, were collected and stored on ice. Reflectance spectra of the samples were measured with an Analytical Spectral Devices (ASD) FieldSpec 3 spectrometer using a contact probe attachment shortly after sampling. Ongoing measurements will characterize the mineralogy of the samples through x-ray diffraction.

Results: Key mineral assemblages are distinguished in the full spectral resolution reflectance data collected with the ASD (Fig. 1). These phases are then connected with NIR hyperspectral imaging data and mapped across the outcrop (Fig. 2).

Reflectance spectra (ASD). Spectra of hydrothermal marcasite (APDI-13-14c) [8, 12] have a broad Fe^{2+} electronic transition absorption centered at 0.8-0.9 µm similar to the 1 µm band reported by [15]. Oxidized marcasite (APDI-13-14j) is visibly red and has an electronic transition centered at slightly longer wavelengths (~0.9 µm), likely due to the presence of Fe^{3+} [e.g., 16]. These spectra also have a strong charge transfer at the shortest wavelengths measured, which is seen as a steep positive slope at 0.35-0.65 µm [e.g., 17]. In the infrared, oxidized marcasite has a negative slope, an H-O-H combination at 1.9 µm, and a weak, broad feature near 2.25 µm, possibly from a sulfate mineral, while unaltered marcasite has a positive infrared slope and lacks the hydration and sulfate bands [e.g., 18-19].

Spectra of mixed sulfates with a botryoidal texture (APDI-13-14a) are dominated by copiapite or fericopiapite and possibly fibroferrite with electronic transitions of Fe^{3+} at 0.42, 0.55, and 0.83 µm and absorption features at 1.77, 1.93, and 2.21 µm, all consistent with Fe^{3+}-sulfates [19]. A dark red coating (APDI-13-14b) shows an electronic transition at 0.91 µm, likely from an Fe^{3+} oxide or sulfate [e.g., 16, 19, 20], as well as a triplet of H_2O overtones and combinations at 1.4-1.5 µm, a vibrational feature at 1.75 µm likely due to H_2O, a deep H-O-H combination band at 1.95 µm, and features at 2.17, 2.22, and 2.27 µm from S-O combinations or OH and H_2O combinations and overtones, all consistent with gypsum [e.g., 19].

Other samples appear to be carbonate and sulfate mixtures. Spectra of a blue-gray phase (APDI-13-14h) have an electronic transition of Fe^{2+} centered near 1.03 µm [e.g., 16]. Absorption features at 2.21 and 2.335 µm could be due to a mixture of a sulfate and Ca-rich carbonate [19, 21]. A tan patch near the top of the exposure (APDI-13-14i) has a similar spectrum with a weak, broad absorption feature near 2.21 µm from an S-O overtone or OH and H_2O combinations and overtones and a stronger feature at 2.34 µm from CO_3 in a Ca-rich carbonate [19, 21]. Combined with a weak triplet at 1.4-1.5 µm and a slight feature at 1.75 µm,

this sample is probably a mixture of calcite and gypsum. Finally, spectra (not shown) of the calcite on which the hydrothermal sulfides and their weathering products precipitated [13] often appear to be gypsum and carbonate mixtures with varying amounts of each phase across the samples. These spectra may result from dissolution of sulfates in the outcrop and subsequent precipitation of gypsum coatings on calcite, although the gypsum and carbonate may be sourced directly from the target rocks [8-9]. Many phases identified at the outcrop by [13] are also identified spectrally here, with exceptions being jarosite and rozenite.

Mapping. Guided by the ASD data, similar mineralogies in the outcrop were mapped with NIR imaging data, and a preliminary map is shown in Fig. 2. Notable in this map is the broad extent of unoxidized marcasite (green), possibly indicating a recent exposure, with patches of more oxidized marcasite. The marcasite and the calcite on which the marcasite precipitated are important because they formed in the post-impact hydrothermal system. Also of interest is the dark red staining often located below the mixed sulfates, which may shed light on more recent, low temperature fluid flow patterns. Together, these observations can be used to understand the post-impact history of this deposit.

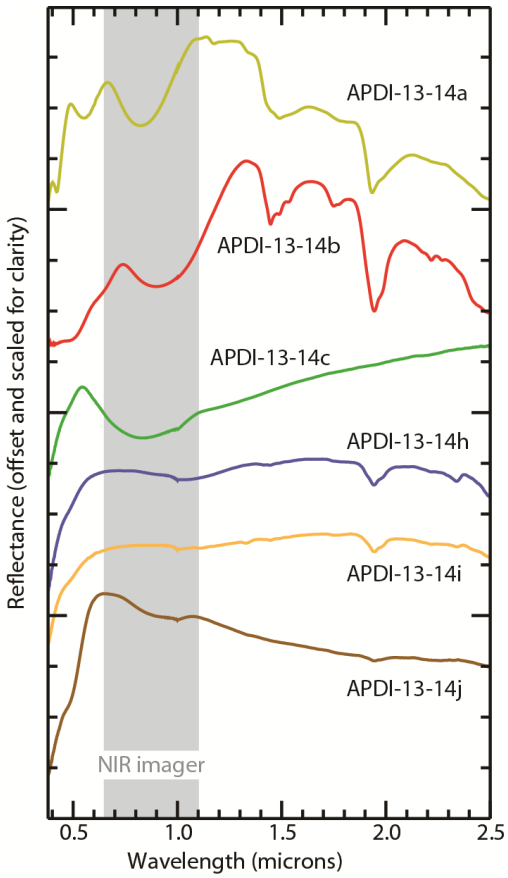

Fig. 1: Reflectance spectra of 6 samples from the outcrop offset and scaled. Sampling locations are shown in Fig. 2. Gray area is the spectral range of the NIR hyperspectral imager.

Conclusions: This hydrothermal vug has a remarkable diversity of mineral assemblages with unique spectral signatures that can be traced across the outcrop in hyperspectral images. The results have implications for understanding how we can detect post-impact hydrothermal mineralization and overprinting of weathering products on Mars and suggest that hyperspectral imaging is a promising technique for future missions to identify and understand hydrothermal deposits.

References: [1] Newsom H. E. (1980), *Icarus, 1,* 207-216. [2] Osinski G. R. et al. (2013), *Icarus, 2,* 347-363. [3] Tornabene L. L. et al. (2009), *LPS XL,* Abstract# 1766. [4] Tornabene L. L. et al. (2013), *JGR, 5,* 994-1012. [5] Marzo G. A. et al. (2011), *Icarus, 2,* 667-683. [6] Schwenzer S. P. and Kring D. A. (2009), *Geol., 37,* 1091-1094. [7] MEPAG E2E-iSAG (2011), *Astrobiology, 12,* 175-230. [8] Osinski G.R. et al. (2005), *Meteoritics & Planet. Sci., 40,* 1859-1877. [9] Osinski G. R. et al. (2005), *Meteoritics & Planet. Sci., 40,*1759-1776. [10] Tornabene L. L. et al. (2005), *Meteoritics & Planet. Sci., 40,* 1-19. [11] Young K. E. et al. (2013), *GRL, 40,* 3836-3840. [12] Osinski G. R. et al. (2001), *Meteoritics & Planet. Sci., 36,*731-745. [13] Izawa M. R. M. (2011), *Astrobiology, 11,* 537-550. [14] Pelkey S. M. et al. (2007), *JGR, 112,* E08S14. [15] Hunt G. R. et al. (1971), *Modern Geol., 3,* 1-14. [16] Burns R. G. (1993), *Cambridge Univ. Press, 2nd ed.,* 578 pp. [17] Burns R. G. (1981), *Ann. Rev. of Earth and Planet. Sci., 9,* 345-383. [18] Clark R. N. et al. (1990), *JGR, 95,* 12653-12680. [19] Cloutis E. A. et al. (2006), *Icarus, 184,* 121-157. [20] Scheinost A. C. (1998), *Clays and Clay Minerals, 46,* 528-536. [21] Hunt G. R. and Salisbury J. W. (1971*), Modern Geol., 2,* 23-30.

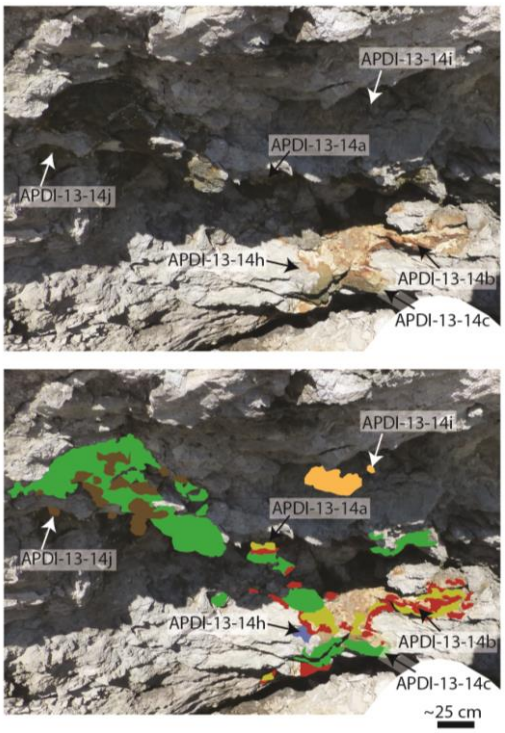

Fig. 2: Photograph of hydrothermal vug outcrop. Top: sampling locations labeled. Bottom: Preliminary mapping of areas that are spectrally-similar to the samples using NIR images and spectral parameters. Colors correspond to spectra in Fig. 1. Green is APDI-13-14c, brown is APDI-13-14j, peach is APDI-13-14i, yellow is APDI-13-14a, red is APDI-13-14b, and blue is APDI-13-14h.